

Article

Novel Mathematical Modelling of Platelet-Poor Plasma Arising in a Blood Coagulation System with the Fractional Caputo–Fabrizio Derivative

Mohammad Partohaghighi ¹, Ali Akgül ^{2,*}, Liliana Guran ³ and Monica-Felicia Bota ^{4,*}¹ Department of Mathematics, Clarkson University, Potsdam, NY 13699, USA; partohm@clarkson.edu² Department of Mathematics, Art and Science Faculty, Siirt University, TR-56100 Siirt, Turkey; aliakgul@siirt.edu.tr³ Department of Pharmaceutical Sciences, “Vasile Goldiș” Western University of Arad, L. Rebreanu Street, No. 86, 310048 Arad, Romania; guran.liliana@uvvg.ro⁴ Department of Mathematics, Babeş-Bolyai University, M. Kogălniceanu Street, No. 1, 400084 Cluj-Napoca, Romania

* Correspondence: aliakgul@siirt.edu.tr (A.A.); monica.bota@ubbcluj.ro (M.-F.B.)

Abstract: This study develops a fractional model using the Caputo–Fabrizio derivative with order α for platelet-poor plasma arising in a blood coagulation system. The existence of solutions ensures that there are solutions to the considered system of equations. Approximate solutions to the recommended model are presented by selecting different numbers of fractional orders and initial conditions (ICs). For each case, graphs of solutions are supplied through different dimensions.

Keywords: Mittag–Leffler kernel; numerical method; blood coagulation model; mathematical modelling; numerical simulation



Citation: Partohaghighi, M.; Akgül, A.; Guran, L.; Bota, M.F. Novel Mathematical Modelling of Platelet-Poor Plasma Arising in a Blood Coagulation System with the Fractional Caputo–Fabrizio Derivative. *Symmetry* **2022**, *14*, 1128. <https://doi.org/10.3390/sym14061128>

Academic Editors: Janusz Brzdek and Eliza Jabłonska

Received: 29 April 2022

Accepted: 28 May 2022

Published: 30 May 2022

Publisher’s Note: MDPI stays neutral with regard to jurisdictional claims in published maps and institutional affiliations.



Copyright: © 2022 by the authors. Licensee MDPI, Basel, Switzerland. This article is an open access article distributed under the terms and conditions of the Creative Commons Attribution (CC BY) license (<https://creativecommons.org/licenses/by/4.0/>).

1. Introduction

Many investigations were conducted on the blood coagulation problem. For example, a numerical investigation of this problem can be seen in [1]. In another work, the conditions of the microvessel occlusion of this problem were reported. A study related to the intrinsic pathway of coagulation and arterial thrombosis is found in [2]. Numerical simulations of the blood coagulation model using the Atangana–Baleanu–Caputo derivative were performed in [3]. Reaction–diffusion waves of blood coagulation was reported in [4]. Moreover, traveling wave solutions in the mathematical model of blood coagulation were found in [5]. The initiation of reaction–diffusion waves of blood coagulation is found in [6]. Blood coagulation is one of the most studied processes in biomedical modeling. This model takes into account patient-specific parameters.

A mathematical model is the explanation of a problem by employing mathematical theories and ideas. Mathematical models are utilized in several branches, such as biology, chemistry, and even art. A model may serve to describe a system, investigate the influences of various elements, and present prognostications about function. Many investigations have been performed in different fields of science.

In recent decades, scientists have devoted specific attention to model different phenomena by using mathematical concepts and tools to analyze the dynamics of intricate problems [7,8]. There are some classical and advanced mathematical instruments that support them to create the behaviors of such problems regarding mathematical patterns. Most such models have been formed using classical mathematical functions, but researchers are now interested to use modern fractional functions to form the models of such different processes. For example, the mathematical modelling of tumor growth can be found in [9,10]. Such a model for chemovirotherapy that describes the effect of infusion scheme can be seen in [11].

Moreover, details of the mathematical model of aortic aneurysm formation are in [12]. More investigations are found in [13–23]. There are some well-known fractional operators to use for modelling phenomena, and the Caputo–Fabrizio fractional operator is one of them. Many investigations involved that operator, such as [24–29]. In this study, we use the Caputo–Fabrizio fractional operator to model platelet-poor plasma arising in a blood coagulation system [30]:

$$\begin{aligned}\frac{dP}{dt} &= -(k_5U(t) + k_6T(t) + k_7T^2(t) + k_8T^3(t))P(t), \\ \frac{dT}{dt} &= (k_5U(t) + k_6T(t) + k_7T^2(t) + k_8T^3(t))P(t) - k_9T(t), \\ \frac{dU}{dt} &= (k_1 + k_2T(t) + k_3T^2(t))(U^0(t) - U(t)) - k_4U^3(t).\end{aligned}\quad (1)$$

Constant k_1 in Equation (1) describes the initiation step. In the above system, P is prothrombin, which is a plasma protein that is turned into thrombin in the closeness of thromboplastin issued with platelets at the locality of damage.

Thrombin T : identified as coagulation constituent II, it is a serine protease that acts as a physiological function in organizing hemostasis and saving blood coagulation. Once switched from prothrombin, thrombin turns fibrinogen into fibrin that, when mixed with platelets from the blood, produces a clot. Thrombin then transforms protein fibrinogen into unsolved fibrin, thereby assisting in blood clotting. Activated factor X or U : a clotting protein or clotting factor. These factors are specific proteins that are necessary for proper clotting, the manner by which blood clusters together to fill the place of an injury to hinder bleeding. This procedure demands a set of responses to eventually produce a clot to fill an injury. Details are provided in [30].

Definition 1. The Caputo–Fabrizio fractional derivative for function $u(t)$ of order α is in the following form [31]:

$${}^{CF}\mathcal{D}_t^\alpha(u(t)) = \frac{(2-\alpha)M(\alpha)}{2(1-\alpha)} \int_0^t \exp\left(\frac{-\alpha}{1-\alpha}(t-z)\right)u'(z)dz, \quad 0 < \alpha \leq 1, \quad (2)$$

$${}^{CF}\ell_t^\alpha(u(t)) = (1-\alpha)u(t) + \alpha \int_0^t u(z)dz, \quad (3)$$

Definition 2. The Caputo–Fabrizio (CF) fractional integral is in the form of the following relation [31]:

$${}^{CF}\mathcal{I}_t^\alpha(u(t)) = \frac{2(1-\alpha)}{(2-\alpha)M(\alpha)}u'(t) + \frac{(2-\alpha)M(\alpha)}{2(1-\alpha)} \int_0^t u'(z)dz, \quad 0 < \alpha \leq 1. \quad (4)$$

Definition 3. The solution of the fractional differential equation in the form of ${}^{CF}\mathcal{D}_t^\alpha(u(t)) = f(t)$ is as follows [31]:

$$u(t) = u(0) + \frac{2(1-\alpha)}{(2-\alpha)M(\alpha)}(u(t) - u(0)) + \frac{2\alpha}{(2-\alpha)M(\alpha)} \int_0^t u(z)dz. \quad (5)$$

Now, we use the above relations to create the fractional model of (1) by changing the classical derivative with a fractional one as follows:

$$\begin{aligned}{}_0^CF\mathcal{D}_t^\alpha P(t) &= -(k_5U(t) + k_6T(t) + k_7T^2(t) + k_8T^3(t))P(t), \\ {}_0^CF\mathcal{D}_t^\alpha T(t) &= (k_5U(t) + k_6T(t) + k_7T^2(t) + k_8T^3(t))P(t) - k_9T(t), \\ {}_0^CF\mathcal{D}_t^\alpha U(t) &= (k_1 + k_2T(t) + k_3T^2(t))(U^0(t) - U(t)) - k_4U^3(t).\end{aligned}\quad (6)$$

Initial conditions (ICs): $P(0) = P_0, T(0) = T_0$, and $U(0) = U_0$. This research is organized as follows. In Section 2, the existence of the resolutions is provided. Then, in Section 3, aspects of the numerical technique utilized to acquire the solutions of the offered model are provided. We present the results and discussion of the current study in Section 4. Lastly, the conclusion of this fractional research is in Section 5.

2. Existence and Uniqueness Results

We supposed the next fractional model to be operating the Caputo–Fabrizio derivative:

$$\begin{cases} {}^{CF}D_0^\alpha P(t) = -(k_5U(t) + k_6T(t) + k_7T^2(t) + k_8T^3(t))P(t), \\ {}^{CF}D_0^\alpha T(t) = (k_5U(t) + k_6T(t) + k_7T^2(t) + k_8T^3(t))P(t) - k_9T(t), \\ {}^{CF}D_0^\alpha U(t) = (k_1 + k_2T(t) + k_3T^2(t))(U^0(t) - U(t)) - k_4U^3(t), \end{cases} \tag{7}$$

with $P(0) = \check{P}_0, T(0) = \check{T}_0$ and $U(0) = \check{U}_0$. To examine the existence of resolutions for the above fractional model, we employed the Picard–Lindelof procedure. We transformed Model (6) into a fractional integral problem.

In fact, we exerted the fractional CF-integral operator stated by Losada and Nieto [32] on both sides of the differential Equation (6); by considering $(P(0), T(0), U(0)) = (\check{P}_0, \check{T}_0, \check{U}_0)$, we have:

$$\begin{aligned} P(t) &= \check{P}_0 + \frac{2(1-\alpha)}{(2-\alpha)M(\alpha)} \left(-(k_5U(t) + k_6T(t) + k_7T^2(t) + k_8T^3(t))P(t) \right) + \\ &\quad \frac{2\alpha}{(2-\alpha)M(\alpha)} \int_0^t \left[-(k_5U(z) + k_6T(z) + k_7T^2(z) + k_8T^3(z))P(z) \right] dz, \\ T(t) &= \check{T}_0 + \frac{2(1-\alpha)}{(2-\alpha)M(\alpha)} \left((k_5U(t) + k_6T(t) + k_7T^2(t) + k_8T^3(t))P(t) - k_9T(t) \right) + \\ &\quad \frac{2\alpha}{(2-\alpha)M(\alpha)} \int_0^t \left[(k_5U(z) + k_6T(z) + k_7T^2(z) + k_8T^3(z))P(z) - k_9T(z) \right] dz, \\ U(t) &= \check{U}_0 + \frac{2(1-\alpha)}{(2-\alpha)M(\alpha)} \left((k_1 + k_2T(t) + k_3T^2(t))(U^0(t) - U(t)) - k_4U^3(t) \right) + \\ &\quad \frac{2\alpha}{(2-\alpha)M(\alpha)} \int_0^t \left[(k_1 + k_2T(z) + k_3T^2(z))(U^0(z) - U(z)) - k_4U^3(z) \right] dz. \end{aligned} \tag{8}$$

Now, considering (8), we used the Picard method by $(n = 0, 1, 2, \dots)$:

$$P_0(t) = \check{T}_0, \quad T_0(t) = \check{T}_0, \quad U_0(t) = \check{U}_0, \tag{9}$$

and:

$$\begin{aligned} P_{n+1}(t) &= \frac{2(1-\alpha)}{(2-\alpha)M(\alpha)} \left(-(k_5U(t) + k_6T(t) + k_7T^2(t) + k_8T^3(t))P(t) \right) + \\ &\quad \frac{2\alpha}{(2-\alpha)M(\alpha)} \int_0^t \left[-(k_5U(z) + k_6T(z) + k_7T^2(z) + k_8T^3(z))P(z) \right] dz, \\ T_{n+1}(t) &= \frac{2(1-\alpha)}{(2-\alpha)M(\alpha)} \left((k_5U(t) + k_6T(t) + k_7T^2(t) + k_8T^3(t))P(t) - k_9T(t) \right) + \\ &\quad \frac{2\alpha}{(2-\alpha)M(\alpha)} \int_0^t \left[(k_5U(z) + k_6T(z) + k_7T^2(z) + k_8T^3(z))P(z) - k_9T(z) \right] dz, \\ U_{n+1}(t) &= \frac{2(1-\alpha)}{(2-\alpha)M(\alpha)} \left((k_1 + k_2T(t) + k_3T^2(t))(U^0(t) - U(t)) - k_4U^3(t) \right) + \\ &\quad \frac{2\alpha}{(2-\alpha)M(\alpha)} \int_0^t \left[(k_1 + k_2T(z) + k_3T^2(z))(U^0(z) - U(z)) - k_4U^3(z) \right] dz. \end{aligned} \tag{10}$$

Taking into account the ideas presented by Li and Zeng in [33], we consider that one can gain the analytic solutions of the system (6) by considering the limit from both sides of (10) whenever n wills to infinity, so the solutions are gained in the following form:

$$\begin{cases} \lim_{n \rightarrow \infty} P_n(t) = P(t), \\ \lim_{n \rightarrow \infty} T_n(t) = T(t), \\ \lim_{n \rightarrow \infty} U_n(t) = U(t), \end{cases} \tag{11}$$

Now, we obtain an existing scale and the uniqueness of the results using the Picard–Lindelof technique. So, we set the next relations:

$$\begin{cases} \Xi_1(t, P) := -(k_5U(t) + k_6T(t) + k_7T^2(t) + k_8T^3(t))P(t), \\ \Xi_2(t, T) := (k_5U(t) + k_6T(t) + k_7T^2(t) + k_8T^3(t))P(t) - k_9T(t), \\ \Xi_3(t, U) := (k_1 + k_2T(t) + k_3T^2(t))(U^0(t) - U(t)) - k_4U^3(t), \end{cases} \tag{12}$$

where $\Xi_1(t, S)$, $\Xi_2(t, L)$ and $\Xi_3(t, R)$ are contractions with respect to P, T and U for the first, second, and third functions.

In addition, we present:

$$\begin{cases} \mathbb{I}_{a,b_1} := [t - a, t + a] \times [P - b_1, P + b_1] = A \times B_1, \\ \mathbb{I}_{a,b_2} := [t - a, t + a] \times [T - b_2, T + b_2] = A \times B_2, \\ \mathbb{I}_{a,b_3} := [t - a, t + a] \times [U - b_3, U + b_3] = A \times B_3, \end{cases} \tag{13}$$

Take $\Xi_1^* = \sup_{(t,P) \in \mathbb{I}_{a,b_1}} \|\Xi_1(t, P(t))\|$, $\Xi_2^* = \sup_{(t,T) \in \mathbb{I}_{a,b_2}} \|\Xi_2(t, T(t))\|$ and $\Xi_3^* = \sup_{(t,U) \in \mathbb{I}_{a,b_3}} \|\Xi_3(t, U(t))\|$.

To apply the Picard technique, let us consider $(\mathcal{C}[t - a, t + a], \mathbb{R})$ to be the space of the real continuous functions defined on $A = [t - a, t + a]$ and a uniform norm defined as follows:

$$\|\mathbb{D}\|_\infty = \sup_{t \in [t-a, t+a]=A} |\mathbb{D}(t)|.$$

It is easy to check that the pair $((\mathcal{C}[t - a, t + a], \mathbb{R}), \|\mathbb{D}\|_\infty)$ it is a complete metric space. Then, we must to put in evidence the symmetry of norm $\|\mathbb{D}\|_\infty$, which is an essential condition in order to prove the existence of a fixed point.

Now, we fix

$$\mathcal{Q} : (\mathcal{C}[t - a, t + a], \mathbb{R}) \rightarrow (\mathcal{C}[t - a, t + a], \mathbb{R}),$$

as

$$\mathcal{Q}(\mathbb{D}(t)) = \mathbb{D}_0(t) + \frac{2(1 - \alpha)}{(2 - \alpha)M(\alpha)} \mathcal{G}(t, \mathbb{D}(t)) + \frac{2\alpha}{(2 - \alpha)M(\alpha)} \int_0^t \mathcal{G}(z, \mathbb{D}(z)) dz, \tag{14}$$

with

$$\begin{cases} \mathbb{D}(t) = \{P(t), T(t), U(t)\}, \\ \mathbb{D}_0(t) = \{\check{P}_0, \check{T}_0, \check{U}_0\}, \\ \mathcal{G}(t, \mathbb{D}(t)) = \{\Xi_1(t, P(t)), \Xi_2(t, T(t)), \Xi_3(t, U(t))\}. \end{cases} \tag{15}$$

All resolution functions were assumed to be limited through a time interval, i.e.,

$$\|\mathbb{D}\|_\infty \leq \max\{b_1, b_2, b_3\} = b. \tag{16}$$

Furthermore, suppose $\Xi^* = \max\{\Xi_1^*, \Xi_2^*, \Xi_3^*\}$, and there is a constant t_0 by $t \leq t_0$. Hence, we obtain

$$\begin{aligned}
 \|Q\mathbb{D}(t) - \mathbb{D}_0(t)\| &= \left\| \frac{2(1-\alpha)}{(2-\alpha)M(\alpha)} \mathcal{G}(t, \mathbb{D}(t)) \right. \\
 &\quad \left. + \frac{2\alpha}{(2-\alpha)M(\alpha)} \int_0^t \mathcal{G}(z, \mathbb{D}(z)) dz \right\| \\
 &\leq \frac{2(1-\alpha)}{(2-\alpha)M(\alpha)} \|\mathcal{G}(t, \mathbb{D}(t))\| \\
 &\quad + \frac{2\alpha}{(2-\alpha)M(\alpha)} \int_0^t \|\mathcal{G}(z, \mathbb{D}(z))\| dz \\
 &\leq \left[\frac{2(1-\alpha)}{(2-\alpha)M(\alpha)} + \frac{2\alpha t_0}{(2-\alpha)M(\alpha)} \right] Y^* \\
 &= \mu^* Y^* \leq b,
 \end{aligned}$$

which we suppose $\mu^* < \frac{b}{Y^*}$, and $\mu^* = \frac{2(1-\alpha)}{(2-\alpha)M(\alpha)} + \frac{2\alpha t_0}{(2-\alpha)M(\alpha)}$.

Lastly, we aim to demonstrate that the Picard operator Q is a contraction. To accomplish this purpose, as Y_1, Y_2 and Y_3 are contractions, for $\mathbb{D}_1, \mathbb{D}_2 \in (C[t - a, t + a], \mathbb{R})$, we have:

$$\|\mathcal{G}(t, \mathbb{D}_1(t)) - \mathcal{G}(t, \mathbb{D}_2(t))\| \leq \lambda^* \|\mathbb{D}_1(t) - \mathbb{D}_2(t)\|, \tag{17}$$

where $\lambda^* < 1$ be a contraction constant.

The Picard operator Q is applied as delivered in (14) using Inequality (17) and the following relation:

$$\|Q\mathbb{D}_1 - Q\mathbb{D}_2\| = \sup_{t \in A} |\mathbb{D}_1(t) - \mathbb{D}_2(t)|,$$

yields:

$$\begin{aligned}
 \|Q(\mathbb{D}_1(t)) - Q(\mathbb{D}_2(t))\| &= \left\| \frac{2(1-\alpha)}{(2-\alpha)M(\alpha)} [\mathcal{G}(t, \mathbb{D}_1(t)) - \mathcal{G}(t, \mathbb{D}_2(t))] + \right. \\
 &\quad \left. \frac{2\alpha}{(2-\alpha)M(\alpha)} \int_0^t [\mathcal{G}(z, \mathbb{D}_1(z)) - \mathcal{G}(z, \mathbb{D}_2(z))] dz \right\| \\
 &\leq \frac{2(1-\alpha)}{(2-\alpha)M(\alpha)} \|\mathcal{G}(t, \mathbb{D}_1(t)) - \mathcal{G}(t, \mathbb{D}_2(t))\| + \\
 &\quad \frac{2\alpha}{(2-\alpha)M(\alpha)} \int_0^t \|\mathcal{G}(z, \mathbb{D}_1(z)) - \mathcal{G}(z, \mathbb{D}_2(z))\| dz \\
 &\leq \frac{2(1-\alpha)\lambda^*}{(2-\alpha)M(\alpha)} \|\mathbb{D}_1(t) - \mathbb{D}_2(t)\| \\
 &\quad + \frac{2\alpha\lambda^*}{(2-\alpha)M(\alpha)} \int_0^t \|\mathbb{D}_1(z) - \mathbb{D}_2(z)\| dz \\
 &\leq \left[\frac{2(1-\alpha)}{(2-\alpha)M(\alpha)} + \frac{2\alpha t_0}{(2-\alpha)M(\alpha)} \right] \lambda^* \|\mathbb{D}_1(t) - \mathbb{D}_2(t)\| \\
 &= \mu^* \lambda^* \|\mathbb{D}_1(t) - \mathbb{D}_2(t)\|.
 \end{aligned}$$

So, this results in

$$\|Q\mathbb{D}_1 - Q\mathbb{D}_2\|_\infty \leq \mu^* \lambda^* \|\mathbb{D}_1 - \mathbb{D}_2\|_\infty,$$

which means that Q is a contraction with $\mu^* \lambda^* < 1$ since $\lambda^* < 1$. Consequently, by applying the Banach contraction principle, we ascertain that fractional System (6) of the blood coagulation model possesses a unique solution.

3. Quadratic Numerical Algorithm

In this section, we use a quadratic numerical approach in order to obtain the approximate solutions of System (6). We turned our Fractional Model (6) into its corresponded integral equation. Next, we used a numerical algorithm based on the trapezoidal ruler to achieve the numerical solutions of the acquired integral equation.

Then, we consider:

$$\begin{cases} {}_0^{\text{CF}}D_t^\alpha \Xi(t) = \Phi(\Xi(t)), 0 \leq t \leq T_f < \infty, \\ \Xi(0) = \Xi_0, \end{cases} \quad (18)$$

where $\Xi(t) = (A(t), B(t), C(t))$, Φ counted as a vector function:

$$\Phi(\Xi(t)) = \begin{bmatrix} -(k_5 U(t) + k_6 T(t) + k_7 T^2(t) + k_8 T^3(t))P(t), \\ (k_5 U(t) + k_6 T(t) + k_7 T^2(t) + k_8 T^3(t))P(t) - k_9 T(t), \\ (k_1 + k_2 T(t) + k_3 T^2(t))(U^0(t) - U(t)) - k_4 U^3(t), \end{bmatrix} \quad (19)$$

which fulfils the Lipschitz condition:

$$\|\Phi(\Xi_1(t)) - \Phi(\Xi_2(t))\| \leq L \|\Xi_1(t) - \Xi_2(t)\|, \quad L > 0, \quad (20)$$

and $\Xi_0 = (P(0), T(0), U(0))$ comprises the ICs. Performing Equation (2) on Equation (18), we obtain:

$$\Xi(t) = \Xi_0 + {}_0^{\text{CF}}\ell_t^\alpha \Phi(\Xi(t)), \quad 0 \leq t \leq T < \infty, \quad (21)$$

We define $0 = t_0 < t_1 < \dots < t_S = T_f$ on $[0, T_f]$ via $h = \frac{T_f}{S} = t_{s+1} - t_s$, where $S > 0$ is an integer, and $t_s = sh, s = 0, 1, 2, \dots, S - 1$.

We use:

$$\Phi(\Xi(\tau))|_{[t_k, t_{k+1}]} \approx \frac{t_{k+1} - \tau}{t_{k+1} - t_k} \Phi(\Xi_k) + \frac{\tau - t_k}{t_{k+1} - t_k} \Phi(\Xi_{k+1}), \quad 0 \leq k \leq s. \quad (22)$$

We have:

$${}_0^{\text{CF}}\ell_t^\alpha \Phi(\Xi(t_{s+1})) = (1 - \alpha) \Phi(\Xi(t_{s+1})) + \alpha \int_0^{t_{s+1}} \Phi(\Xi(\tau)) d\tau. \quad (23)$$

Replacing Equation (22) into Equation (23) results in

$$\Xi_{s+1} = \Xi_0 + (1 - \alpha) \Phi(\Xi_{s+1}) + \alpha h \sum_{k=0}^{s+1} a_{s+1,k} \Phi(\Xi_k), \quad s = 0, 1, \dots, S - 1, \quad (24)$$

where coefficient $a_{s+1,k}$ is in the following form:

$$\begin{cases} a_{s+1,0} = \frac{1}{2}, \\ a_{s+1,k} = 1, \\ a_{s+1,s+1} = \frac{1}{2}, \end{cases} \quad k = 1, 2, \dots, s. \quad (25)$$

4. Numerical Examples

Now, we use the stated numerical method as provided in the previous section to obtain the approximate solutions of the platelet-poor plasma system as recommended in the current investigation under the fractional Caputo–Fabrizio operator. All simulations were plotted in MATLAB version 2021. We solves the model for various numbers of fractional order α .

The following parameters were used in the studied model: $k_1 = 1.5, k_2 = 1.5, k_3 = 0.5, k_4 = 0.5, k_5 = 0.5, k_6 = 0.5, k_7 = 0.5, k_8 = 0.5$ and $k_9 = 0.5$. Approximate solutions of

the considered model under fractional orders of 0.75, 0.85, 0.95, and 1 with ICs given as $P(0) = 1500$, $T(0) = 500$ and $U(0) = 300$ are provided in Figure 1.

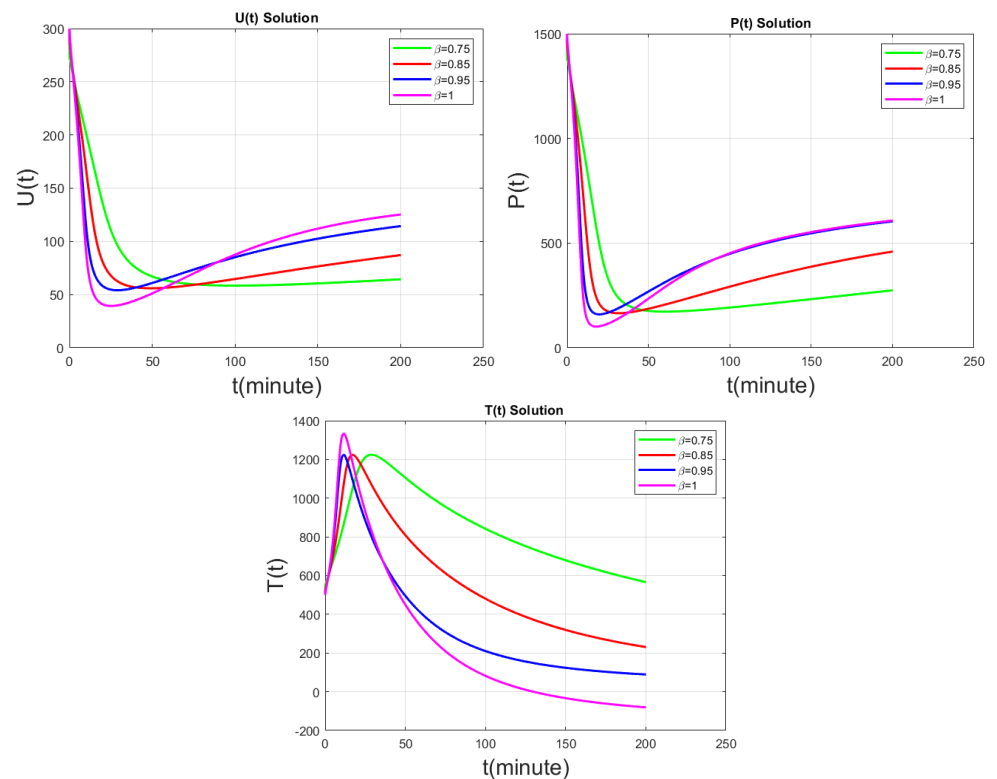


Figure 1. Plot of solutions for different values of α with ICs $P(0) = 1500$, $T(0) = 500$ and $U(0) = 300$.

In Figure 1, the line graph illustrates the changing trends in the amounts of prothrombin, thrombin, and the activated factor. According to the graph, the numerical simulation of prothrombin $P(t)$ experienced a sharp decrease and fell to a low point of approximately 100 in the 25th minute, and then increased moderately throughout the time frame of 200 min. The rate of decline was different for each fractional order. A fairly similar pattern over the 200 min under various values of the fractional orders was seen. A similar trend was seen for $U(t)$ with an initial value of 300, which experienced a sudden decrease, reaching its minimal amount in 25 min; after that, it showed a gradual increase reaching the maximal value in 200 min.

In contrast, $T(t)$ showed a different pattern. The provided graph shows that $T(t)$ with an initial value of 600 began with a sharp increase, reaching its peak around 1300. After that, it began to fall for the rest of the time frame of 200 min. It is clear that the rate of increase depended on the values of the fractional orders.

Figure 2 shows the approximate solutions of the problem under different ICs of $P(0) = 700$, $T(0) = 2100$ and $U(0) = 500$. In this case, similar behaviors were seen for $U(t)$ and $P(t)$.

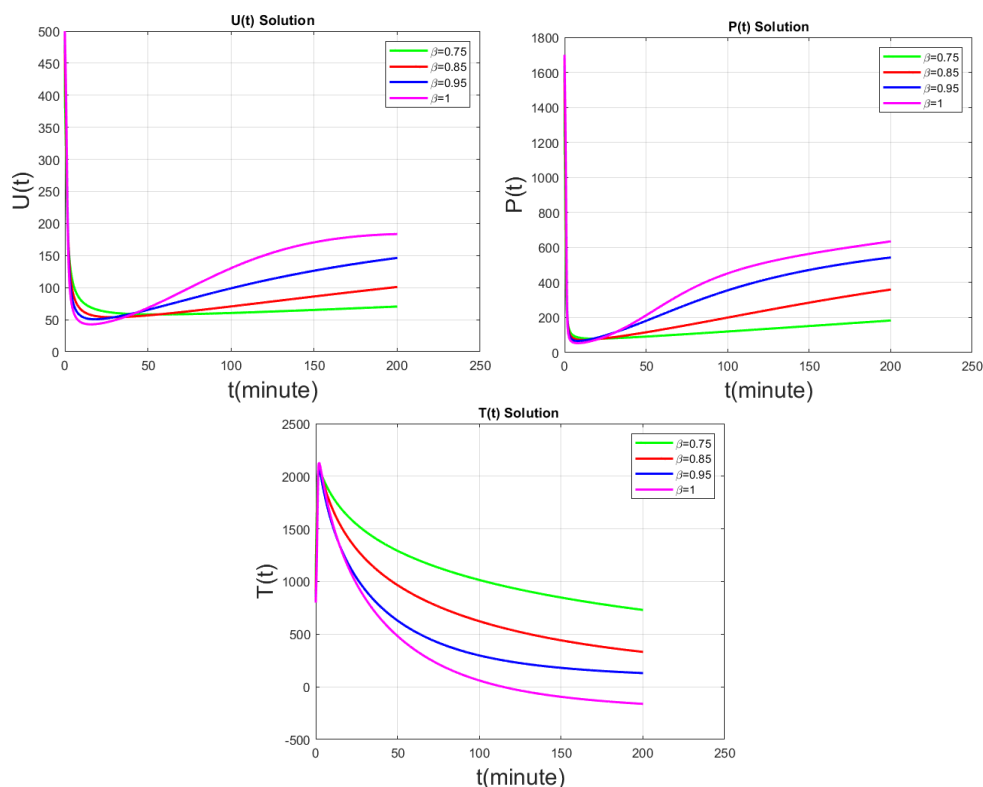


Figure 2. Plot of solutions α with ICs $P(0) = 700$, $T(0) = 2100$ and $U(0) = 500$.

5. Conclusions

In this work, the fractional modelling of a blood coagulation system was investigated for the first time by applying a fractional derivative of the frame Caputo–Fabrizio operator, and the existence of solutions was given. A numerical method to obtain approximate solutions was also derived. Moreover, numerical solutions of the proposed model are presented through some graphical representations. These figures contain simulations of the problem for different values of fractional orders. We provided solutions by separately choosing two ICs. Behaviors of the offered model were obvious during the selection of various values of orders and initial conditions.

Author Contributions: Conceptualization, M.P., A.A. and L.G.; methodology, A.A.; software, M.P.; validation, M.P., A.A. and M.-F.B.; formal analysis L.G.; investigation, M.P.; resources, M.-F.B.; writing—original draft preparation, M.P.; writing—review and editing, L.G.; visualization, M.-F.B.; supervision, A.A.; project administration, A.A.; funding acquisition, M.-F.B. All authors have read and agreed to the published version of the manuscript.

Funding: This research received no external funding.

Institutional Review Board Statement: Not applicable.

Informed Consent Statement: Not applicable.

Data Availability Statement: Not applicable.

Acknowledgments: The authors would like to thank Babeş-Bolyai University of Cluj-Napoca for financial support.

Conflicts of Interest: The authors declare no conflict of interest.

References

1. Karasu, S.; Altan, A.; Bekiros, S.; Ahmad, W. A new forecasting model with wrapper-based feature selection approach using multi-objective optimization technique for chaotic crude oil time series. *Energy* **2020**, *212*, 118750. [[CrossRef](#)]
2. Xu, S.; Bai, M. Stability of solutions to a mathematical model for necrotic tumor growth with time delays in proliferation. *J. Math. Anal. Appl.* **2015**, *421*, 955–962. [[CrossRef](#)]
3. Pang, L.; Shen, L.; Zhao, Z. Mathematical modelling and analysis of the tumor treatment regimens with pulsed immunotherapy and chemotherapy. *Comput. Math. Methods Med.* **2019**, *2016*, 6260474. [[CrossRef](#)]
4. Malinzi, J. Mathematical analysis of a mathematical model of chemovirotherapy: Effect of drug infusion method. *Comput. Math. Methods Med.* **2019**, *2019*, 7576591. [[CrossRef](#)] [[PubMed](#)]
5. Hao, W.; Gong, S.; Wu, S.; Xu, J.; Go, M.R.; Friedman, A.; Zhu, D. A mathematical model of aortic aneurysm formation. *PLoS ONE* **2017**, *12*, e0170807. [[CrossRef](#)] [[PubMed](#)]
6. Gómez-Aguilar, J. Chaos and multiple attractors in a fractal–fractional Shinriki’s oscillator model. *Phys. A Stat. Mech. Appl.* **2020**, *539*, 122918. [[CrossRef](#)]
7. Gómez-Aguilar, J. Multiple attractors and periodicity on the Vallis model for El Niño/La Niña–Southern oscillation model. *J. Atmos. Sol.-Terr. Phys.* **2020**, *197*, 105172. [[CrossRef](#)]
8. Hoan, L.V.C.; Akinlar, M.A.; Inc, M.; Gómez-Aguilar, J.; Chu, Y.M.; Almohsen, B. A new fractional-order compartmental disease model. *Alex. Eng. J.* **2020**, *59*, 3187–3196. [[CrossRef](#)]
9. Naik, P.A.; Zu, J.; Owolabi, K.M. Global dynamics of a fractional order model for the transmission of HIV epidemic with optimal control. *Chaos Solitons Fractals* **2020**, *138*, 109826. [[CrossRef](#)]
10. Valle, P.A.; Coria, L.N.; Gamboa, D.; Plata, C. Bounding the dynamics of a chaotic-cancer mathematical model. *Math. Probl. Eng.* **2018**, *2018*, 9787015. [[CrossRef](#)]
11. Qureshi, S.; Atangana, A. Fractal-fractional differentiation for the modeling and mathematical analysis of nonlinear diarrhea transmission dynamics under the use of real data. *Chaos Solitons Fractals* **2020**, *136*, 109812. [[CrossRef](#)]
12. Khan, A.; Abdeljawad, T.; Gómez-Aguilar, J.; Khan, H. Dynamical study of fractional order mutualism parasitism food web module. *Chaos Solitons Fractals* **2020**, *134*, 109685. [[CrossRef](#)]
13. Singh, J.; Kumar, D.; Hammouch, Z.; Atangana, A. A fractional epidemiological model for computer viruses pertaining to a new fractional derivative. *Appl. Math. Comput.* **2018**, *316*, 504–515. [[CrossRef](#)]
14. Kumar, S.; Kumar, A.; Argyros, I.K. A new analysis for the Keller–Segel model of fractional order, Numer. *Algorithms* **2017**, *75*, 213–228. [[CrossRef](#)]
15. Abdullah, M.; Ahmad, A.; Raza, N.; Farman, M.; Ahmad, M.O. Approximate solution and analysis of smoking epidemic model with Caputo fractional derivatives. *Int. J. Appl. Comput. Math.* **2018**, *4*, 112. [[CrossRef](#)]
16. Kumara, D.; Singha, J.; Baleanu, D. A new analysis for fractional model of regularized long-wave equation arising in ion acoustic plasma waves. *Math. Methods Appl. Sci.* **2017**, *40*, 5642–5653. [[CrossRef](#)]
17. Abdo, M.S.; Shah, K.; Wahash, H.A.; Panchal, S.K. On a comprehensive model of the novel coronavirus (COVID-19) under Mittag–Leffler derivative. *Chaos Solitons Fractal* **2020**, *135*, 109867. [[CrossRef](#)]
18. Alizadeh, S.; Baleanu, D.; Rezapour, S. Analyzing transient response of the parallel RCL circuit by using the Caputo–Fabrizio fractional derivative. *Adv. Differ. Equ.* **2020**, *2020*, 55. [[CrossRef](#)]
19. Alsaedi, A.; Baleanu, D.; Etemad, S.; Rezapour, S. On coupled systems of timefractional differential problems by using a new fractional derivative. *J. Funct. Spaces* **2016**, *2016*, 4626940. [[CrossRef](#)]
20. Aydogan, M.S.; Baleanu, D.; Mohammadi, H.; Rezapour, S. On the mathematical model of rabies by using the fractional Caputo–Fabrizio derivative. *Adv. Differ. Equ.* **2020**, *2020*, 382. [[CrossRef](#)]
21. Aydogan, M.S.; Baleanu, D.; Mousalou, A.; Rezapour, S. On approximate solutions for two higher-order Caputo–Fabrizio fractional integro-differential equations. *Adv. Differ. Equ.* **2017**, *2017*, 221. [[CrossRef](#)]
22. Aydogan, M.S.; Baleanu, D.; Mousalou, A.; Rezapour, S. On high order fractional integro-differential equations including the Caputo–Fabrizio derivative. *Bound. Value Probl.* **2018**, *2018*, 90. [[CrossRef](#)]
23. Baleanu, D.; Mohammadi, H.; Rezapour, S. A fractional differential equation model for the COVID-19 transmission by using the Caputo–Fabrizio derivative. *Adv. Differ. Equ.* **2020**, *2020*, 299. [[CrossRef](#)] [[PubMed](#)]
24. Baleanu, D.; Mousalou, A.; Rezapour, S. A new method for investigating approximate solutions of some fractional integro-differential equations involving the Caputo–Fabrizio derivative. *Adv. Differ. Equ.* **2017**, *2017*, 51. [[CrossRef](#)]
25. Baleanu, D.; Mousalou, A.; Rezapour, S. The extended fractional Caputo–Fabrizio derivative of order $0 \leq \sigma < 1$ in $R[0, 1]$ and the existence of solutions for two higher-order series-type differential equations. *Adv. Differ. Equ.* **2018**, *2018*, 255.
26. Dokuyucu, M.A.; Celik, E.; Bulut, H.; Baskonus, H.M. Cancer treatment model with the Caputo–Fabrizio fractional derivative. *Eur. Phys. J. Plus* **2018**, *133*, 92. [[CrossRef](#)]
27. Khan, S.A.; Shah, K.; Zaman, G.; Jarad, F. Existence theory and numerical solutions to smoking model under Caputo–Fabrizio fractional derivative. *Chaos* **2019**, *29*, 013128. [[CrossRef](#)]
28. Shah, K.; Abdeljawad, T.; Mahariq, I.; Jarad, F. Qualitative analysis of a mathematical model in the time of COVID-19. *BioMed Res. Int.* **2020**, *2020*, 5098598. [[CrossRef](#)]
29. Shah, K.; Alqudah, M.A.; Jarad, F.; Abdeljawad, T. Semi-analytical study of pine wilt disease model with convex rate under Caputo–Fabrizio fractional order derivative. *Chaos Solitons Fractal* **2020**, *135*, 109754. [[CrossRef](#)]

30. Ratto, N.; Bouchnita, A.; Chelle, P.; Marion, M.; Panteleev, M.; Nechipurenko, D.; Tardy-Poncet, B.; Volpert, V. Patient-Specific Modelling of Blood Coagulation. *Bull. Math. Biol.* **2021**, *83*, 50. [[CrossRef](#)]
31. Caputo, M.; Fabrizio, M. A new definition of fractional derivative without singular kernel. *Prog. Fract. Differ. Appl.* **2015**, *1*, 73–85.
32. Losada, J.; Nieto, J.J. Properties of the new fractional derivative without singular kernel. *Prog. Fract. Differ. Appl.* **2015**, *1*, 87–92.
33. Li, C.; Zeng, F. The finite difference methods for fractional ordinary differential equations. *Numer. Funct. Anal. Optim.* **2013**, *34*, 149–179. [[CrossRef](#)]